JOURNAL OF SOLID STATE CHEMISTRY 52, 12–21 (1984)

Crystal Structures and Magnetic Properties of $BaTiF_5$ and $CaTiF_5$

S. M. EICHER AND J. E. GREEDAN

Institute for Materials Research and Department of Chemistry, McMaster University Hamilton, Ontario L8S 4M1, Canada

Received August 15, 1983; in revised form October 21, 1983

Single crystals of $BaTiF_5$ and $CaTiF_5$ were obtained by the Czochralski and Bridgman techniques, respectively. The crystal structures were determined by X-ray diffraction; $BaTiF_5$: $I4/m$, a = 15.091(5) Å, c = 7.670(3) Å; $CaTiF_5$: $I2/c$, a = 9.080(4) Å, b = 6.614 Å, c = 7.696(3) Å, β = 115.16(3)°. Both structures are characterized by the presence of either branched or straight chains of TiF_6 octahedra. $BaTiF_5$ contains the unusual dimeric unit $(Ti_2F_{10})^{4-}$. Magnetic susceptibility measurements were performed on both compounds in the temperature range 4.2 to 300 K, however, no evidence for magnetic interactions between the Ti^{3+} moments were observed.

Introduction

Materials with the general formula ABF_5 (where A = divalent transition metal ion or alkaline earth ion and B = trivalent transition metal ion) have been extensively investigated (see (*1–6*) and references therein). The details of the crystal structures of these phases are found to vary, however they are all characterized by the presence of isolated chains of magnetic ions $(BF_5)_n^{2n-}$. This feature of their structure makes these compounds interesting model systems for studying magnetic interactions in one dimension.

As part of an investigation of systems displaying magnetism in less than three dimensions the compounds $ATiF_5$ (A = Ca, Ba) were prepared and single-crystal X-ray studies were performed. Magnetic susceptibility measurements were obtained in the temperature range 4.2 to 300 K.

Experimental

(*i*) *Preparation and crystal growth.* $BaTiF_5$ and $CaTiF_5$ were prepared by solid state reaction of equimolar mixtures of the binary fluorides. TiF_3 was purified by vacuum sublimation. Commercially available BaF_2 (Alfa Products, ultrapure) and CaF_2 (Allied Chemicals) were used without further treatment. The reaction mixtures were sealed in Ni-crucibles under ca. 0.5 atm Ar and then fired at ca. 800°C for several days.

Single crystals of $BaTiF_5$ were grown from the melt in an Ar atmosphere by the Czochralski method. The crystal was pulled at a rate of 1 cm/hr and neither the crucible (Ni) nor the seed rod (Pt–Rh wire) were rotated. Examination of the boule by Laue techniques revealed the presence of relatively large single-crystal areas (10 mm^3). Thin sections or powdered specimens of $BaTiF_5$ were dark purple in color.

0022-4596/84 $3.00

TABLE I

CRYSTAL DATA FOR $CaTiF_5$ AND $BaTiF_5$

	$BaTiF_5$	$CaTiF_5$
Formula weight (g/mole)	280.23	182.98
Crystal size	Sphere, $r = 0.017$ cm	$0.020 \times 0.020 \times 0.016$ cm^3
Systematic absences	$h + k + l = 2n$	$h + k + l = 2n$
Space group	$I4/m$	$I2/c$
Unit cell parameters	$a = 15.091(5)$	$a = 9.080(4)$ $b = 6.614(2)$
	$c = 7.670(3)$	$c = 7.696(3)$ $\beta = 115.16(3)°$
V (Å^3)	1747(1)	418.4(3)
Z	16	4
d_{calc} (g/cm^3)	4.26	2.90
d_{obs} (g/cm^3)	4.20(3)	2.66(5)
Linear abs. coeff. (cm^{-1})	112	33
Std. refl. (% esd)	$\bar{6}\,3\,\bar{1}$ (1.08), $\bar{6}\,1\,\bar{1}$ (1.14)	$3\,\bar{3}\,2$ (0.95), $\bar{2}\,\bar{1}\,\bar{3}$ (0.94)
No. independent refl.	1084	463
Final R,[a] R_w[b]	0.0332, 0.0355	0.0177, 0.0211
g (2° extinction)	3.1×10^{-4}	6.85×10^{-3}
Weighting (w)	$1/\sigma^2$	$1/\sigma^2$
Unit weights	3.5522	1.2563

[a] $R = \dfrac{\Sigma(|F_0| - |F_c|)}{\Sigma|F_0|}$

[b] $R_w = \dfrac{\Sigma\sqrt{w}(|F_0| - |F_c|)}{\Sigma\sqrt{w}|F_0|}$

In the case of $CaTiF_5$ it was found that the stoichiometric melt of the binary fluorides was too volatile to grow crystals by the Czochralski method. Single crystals of $CaTiF_5$ were obtained from a Bridgman growth in a sealed Mo crucible at a cooling rate of approximately 15 K/hr. Some of the larger grains in the boule measured ca. 5–6 mm^3. The crystals were quite clear and their color changed with the direction of the viewing angle: in one direction the crystals appeared pale green, in the other: red–brown.

(*ii*) *Crystallographic study and data collection.* Small single crystals (Table I) were selected for data collection. Precession photographs gave the crystal classes and the observed systematic absences allowed the assignment of space groups. In the case of $BaTiF_5$ precession photographs were taken with long exposure times (10 days) to determine whether doubling along the c-axis had occurred; however, no reflections of the type $h\,k\,\frac{l}{2}$ were observed. Accurate unit cell parameters were obtained by least-squares refinement of 15 well-centered reflections in the range $21 < 2\theta < 38$ ($BaTiF_5$) and $20 < 2\theta < 30$ ($CaTiF_5$). Intensity measurements were performed on a Nicolet P3 four circle diffractometer in the $\theta/2\theta$ scan mode, using Mo$K\alpha$ radiation ($\lambda = 0.71069$ Å). Two reflections were measured at regular intervals for both compounds, and they showed no significant variation in intensity.

(*iii*) *Solution of structures.* The observed intensities were corrected for Lorentz and polarization effects, as well as for secondary extinction (*7*). Atomic scattering curves for free ions were taken from Cromer and Waber (*8a*) and anomalous dispersion coefficients were obtained from Cromer (*8b*). Absorption corrections were applied by the PSI-scan method. No significant changes in

TABLE II

ATOMIC COORDINATES AND ANISOTROPIC THERMAL PARAMETERS ($\times 10^4$)[a] FOR $BaTiF_5$

	X	Y	Z	U_{11}	U_{22}	U_{33}	U_{23}	U_{13}	U_{12}
Ba1	2490(0)	716(0)	0	139(3)	156(3)	130(3)	0	0	−29(2)
Ba2	2842(0)	5547(0)	0	100(3)	117(3)	152(3)	0	0	18(2)
Ti1	0	0	2144(3)	87(7)	87(7)	125(11)	0	0	0
Ti2	0	½	0	136(12)	154(12)	109(11)	0	0	11(10)
Ti3	1670(1)	3174(1)	0	99(8)	85(5)	114(8)	0	0	−10(6)
F1	1055(3)	2423(3)	1702(6)	488(31)	461(31)	159(22)	97(21)	−5(22)	−225(26)
F2	2153(3)	4014(3)	1688(5)	414(28)	254(24)	153(21)	−14(18)	−45(19)	−106(21)
F3	1176(5)	492(6)	2273(12)	149(43)	245(47)	308(49)	59(39)	38(36)	−31(36)
F4	1092(4)	5678(4)	0	131(31)	181(32)	620(49)	0	0	−9(26)
F5	0	½	¼	422(34)	422(34)	200[b]	0	0	0
F6	527(5)	3817(5)	337[b]	161(34)	136(33)	389(74)	12(40)	25(41)	25(27)
F7	2751(4)	2439(4)	0	151(30)	200(31)	421(39)	0	0	33(25)
F8	921(6)	465(5)	3669(11)	232(45)	167(43)	303(49)	−51(37)	−96(39)	11(36)
F9	771(7)	318(8)	0	87(56)	291(70)	388(75)	0	0	−56(52)

[a] Standard deviations are given in parentheses.

[b] These values were fixed in the final stages of refinement.

the intensities were observed, consistent with the fact that $\mu R < 2$ for both crystals.

In the early stages of refinement of $BaTiF_5$ the structure reported for $BaFeF_5$, space group *I*4 (*3*), was taken as a model. Refinement of the Ba and Ti positions led to $R = 0.15$. The positions of the fluorine atoms F1, F2, F4, F5, F6, and F7 were then found from three-dimensional electron density difference syntheses. In the further course of the refinement it was noticed that pairs of atoms were related by a center of symmetry. The observation of strong correlations in the z-parameters of these atoms confirmed the presence of a center of symmetry and led to the adoption of the centric space group *I*4/*m*.

Attempts to place a bridging fluorine between the two Ti atoms on the fourfold axis (cf. F(1) and F(2) in $BaFeF_5$ (*3*)) were unsuccessful, instead the electron density difference maps gave strong peaks in the positions: 0.07, 0.03, 0 (F9), 0.09, 0.05, 0.36 (F8), and 0.12, 0.05, 0.22 (F3). Subsequent refinement showed that each of these sites was only half-occupied, indicating rotational disorder of F3, F8, and F9 around the fourfold axis. These fluorine positions and the observation that the Ti–Ti distance within the unit cell (3.288(3) Å) differs considerably from the Ti–Ti distance between two unit cells (4.381(4) Å) are not consistent with linear chains of TiF_6 octahedra, but rather they point toward the presence of edge-sharing $(Ti_2F_{10})^{4-}$ dimers (Fig. 4). The atomic coordinates and anisotropic thermal parameters of all atoms were refined in the space group *I*4/*m* to a final R-value of 0.0332 ($R_w = 0.0355$). The final atomic positions and anisotropic thermal parameters are given in Table II; interatomic distances and angles are listed in Table III.

The refinement of the structure of $CaTiF_5$ followed a similar course, taking $CaCrF_5$, *C*2/*c* (*5*, *6*) and $MnCrF_5$, *C*2/*c* (*9*) as models. The starting values for the positional parameters were taken from these structures; however, the structure of $CaTiF_5$ was refined in the nonstandard space group *I*2/*c*. The unit cell of the nonstandard body-centered space group can be transformed to the corresponding standard

C-centered unit cell by the following matrix:

$$\begin{pmatrix} a_c \\ b_c \\ c_c \end{pmatrix} = \begin{pmatrix} 1 & 0 & 1 \\ 0 & -1 & 0 \\ 0 & 0 & -1 \end{pmatrix} \begin{pmatrix} a_I \\ b_I \\ c_I \end{pmatrix}$$

$a_c = 9.070$ Å $\quad a_I = 9.080$ Å,

$b_c = b_I$

$c_c = c_I$

The fluorine atomic positions were again located from electron density difference syntheses. Refinement of all atomic positions and anisotropic thermal parameters resulted in a final R-value of 0.0177 (R_w = 0.0211). Tables IV and V summarize the crystallographic information for $CaTiF_5$.[1]

(*iv*) *Magnetic susceptibility*. These measurements were performed on a vibrating sample magnetometer over the temperature range 4.2 to 300 K. Each sample was checked for spontaneous moments at 4.2 K but none were observed. This indicates that the samples are paramagnetic and also confirms the absence of significant amounts of ferromagnetic impurities (e.g., Ni). The measured susceptibility was corrected for the diamagnetism of the ion cores. The variation of the inverse of the magnetic susceptibility for both compounds is shown in Fig. 1. These curves were fitted to a Curie–Weiss law with a temperature-independent term (χ_{TIP}):

$$\chi = \frac{C}{T - \theta} + \chi_{TIP}$$

[1] See NAPS document No. 04150 for 8 pages of supplementary material. Order from ASIS/NAPS, Microfiche Publications, P.O. Box 3513, Grand Central Station, New York, NY 10163. Remit in advance $4.00 for microfiche copy or for photocopy, $7.75 up to 20 pages plus $.30 for each additional page. All orders must be prepaid. Institutions and organizations may order by purchase order. However, there is a billing and handling charge for this service of $15. Foreign orders add $4.50 for postage and handling, for the first 20 pages, and $1.00 for additional 10 pages of material. Remit $1.50 for postage of any microfiche orders.

TABLE III

BOND LENGTHS (Å) AND BOND ANGLES (deg) FOR $BaTiF_5$

		Chain	
Ti2–F4	1.940(6)	F4–Ti2–F5	90.00(0)
F5	1.918(0)	F4–Ti2–F6	82.27(.28)
F6	1.972(7)	F5–Ti2–F6	82.48(.03)
			97.52(.03)
		Ti2–F6–Ti3	140.55(.36)
Ti3–F1	1.961(5)	F1–Ti3–F6	77.62(.22)
F2	1.953(4)		87.59(.22)
F6	1.995(7)	F1–Ti3–F7	93.84(.21)
F7	1.973(6)	F2–Ti3–F6	85.47(.22)
			95.32(.22)
		F2–Ti3–F7	93.21(.20)
		Dimer	
Ti1–Ti1	3.288(3)	F3–Ti1–F3′	174.12(.40)
Ti1–F3	1.926(8)	F3–Ti1–F8	84.95(.36)
F8	1.948(9)	F3–Ti1–F8′	91.51(.37)
F9	2.070(7)	F3–Ti1–F9	92.19(.43)
		F3–Ti1–F9′	92.48(.43)
F9–F9′	2.517(16)	F8–Ti1–F8′	106.18(.38)
		F8–Ti1–F9	89.56(.36)
		F9–Ti1–F9′	74.86(.36)
		Ti1–F9–Ti1	105.14(.50)

Note. Standard deviations given in parentheses.

The fitting parameters are listed in Table VI.

(*v*) *Differential scanning calorimetry* (*DSC*). These measurements were carried out on a DuPont DTA 900 instrument

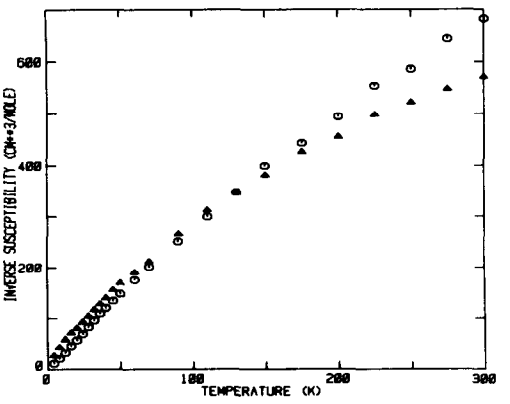

FIG. 1. Inverse susceptibility vs T for $BaTiF_5$ (△) and $CaTiF_5$ (○).

TABLE IV

ATOMIC COORDINATES AND ANISOTROPIC THERMAL PARAMETERS FOR $CaTiF_5$ ($\times 10^4$)[a]

	X	Y	Z	U_{11}	U_{22}	U_{33}	U_{23}	U_{13}	U_{12}
Ca	0	5418(1)	¼	104(3)	94(2)	101(3)	0	39(2)	0
Ti	0	0	0	91(2)	84(2)	82(2)	3(1)	33(2)	3(1)
F1	0	9096(2)	¼	321(10)	141(7)	130(8)	0	137(7)	0
F2	111(1)	7007(1)	5420(2)	278(7)	96(5)	154(6)	18(4)	114(5)	2(4)
F3	−2289(1)	9794(2)	3893(2)	108(6)	314(7)	289(7)	−18(5)	45(5)	−12(5)

[a] Standard deviations given in parentheses.

equipped with a high temperature furnace. Samples of $BaTiF_5$ were placed in Pt boats and heated at 20°C/min in an atmosphere of Ar; the reference material was Al_2O_3. Over the temperature range studied (25–950°C) the only thermal event observed was the melting point at 890 ± 20°C.

TABLE V

INTERATOMIC DISTANCES (Å) AND BOND ANGLES (deg)[a]

Ca–Environment		
Ca–F2(3)	2.299(1)	
F2(4)	2.299(1)	
F1(1)	2.433(2)	
F2(2)	2.444(1)	
F2(1)	2.444(1)	
F3(7)	2.233(1)	
F3(8)	2.233(1)	
F1(1)–Ca–F2(1)		64.54(3)
F2(2)–Ca–F2(4)		69.90(4)
F2(3)–Ca–F2(4)		91.50(5)
F3(8)–Ca–F1(1)		93.61(3)
F3(8)–Ca–F2(1)		88.84(4)
F3(8)–Ca–F2(4)		85.68(4)
Ti–Environment		
Ti–F1(1)	2.015(1)	
F1(3)	2.015(1)	
F2(2)	2.002(1)	
F2(4)	2.002(1)	
F3(2)	1.886(1)	
F3(4)	1.886(1)	
F1(1)–Ti–F2(2)		80.81(5)
F1(1)–Ti–F3(2)		89.69(4)
F2(2)–Ti–F3(2)		88.38(5)
Ti(1)–F1(1)–Ti(2)		145.48(8)

[a] Standard deviations given in parentheses.

Description of Structures

(*i*) *$BaTiF_5$*. The structure of $BaTiF_5$ is closely related to that reported for $BaFeF_5$ but, apparently, the two compounds are not isostructural. A comparison of their unit cell constants is given in Table VII. Both structures are made up of different units with the general formula $(BF_5)_n^{2n-}$ (B = Fe,Ti).

The first of these building blocks is the same in both compounds and consists of a straight chain of corner-sharing octahedra propagating parallel to the c-axis at $0,\frac{1}{2},z$ and $\frac{1}{2},0,z$ (Fig. 3). At $z = 0$ and $z = \frac{1}{2}$ two opposite, equatorial fluorine atoms have been replaced by BF_6 octahedra, giving rise to branched chains. The relative orientation of these "satellites" at $z = 0$ and $z = \frac{1}{2}$ is approx. 90° (Fig. 2). The branched chain can be represented by $(BF_5(BF_5)_2)_n^{2n-}$ where $n = \infty$. In this chain Ti^{3+} ions are found in two different environments: Ti2 in

TABLE VI

MAGNETIC SUSCEPTIBILITY DATA[a] FOR $CaTiF_5$ AND $BaTiF_5$

	$CaTiF_5$	$BaTiF_5$
$C\left(\frac{cm^3K}{mole}\right)$	0.345(13)	0.200(13)
μ_{eff} (μ_B)	1.66(6)	1.26(8)
θ (K)	0.21(5)	−1.2(4)
$\chi_{TIP}\left(\frac{cm^3}{mole}\right)$	$3(3) \times 10^{-4}$	$1.9(3) \times 10^{-3}$

[a] Standard deviation given in parentheses.

TABLE VII

COMPARISON OF UNIT CELL PARAMETERS

CMPD	Space group	*a* (Å)	*b* (Å)	*c* (Å)	β	Reference
$BaFeF_5$	*I*4	14.919 ± .002	—	7.609 ± .02[a]		(*3*)
$BaTiF_5$	*I*4/*m*	15.091(5)		7.670(3)		This work
$MnCrF_5$	*C*2/*c*	8.586(5)	6.291(3)	7.381(4)	115.46(7)	(*9*)
$CaCrF_5$	*C*2/*c*	9.005(5)	6.472(5)	7.533(5)	115.85(10)	(*6*)
	Cc	9.005(5)	6.472(5)	7.533(5)	115.85(10)	(*5*)
$CaTiF_5$	*I*2/*c*	9.080(4)	6.614(2)	7.696(3)	115.16(3)	This work

[a] A slight distortion along the *c*-axis results in a superlattice with space group *P*4 and $c' = 15.21_8 \pm .02$.

the backbone of the chain and Ti3 in the satellites. Both can be described as distorted octahedra (Table III). The bond lengths (l) are all in the range $1.917 \leq l \leq 1.992$ and are consistent with the sum of the ionic radii (1.97 Å (*10*)). The bridging fluorine F6, has moved off the special position $x,y,0$ to the general position $x,y,0.0337$, causing the octahedron around Ti2 to be more distorted than expected on the basis of the site symmetry (2/*m*).

The second building block in the structure of $BaTiF_5$ is formed by two TiF_6 octahedra sharing an edge to give the dimer $(Ti_2F_{10})^{4-}$. This coordination environment is quite unusual for Ti^{3+} and the dimers represent the unique feature of this structure (Fig. 4). Halide-bridged dimers with the formula $((C_5H_5)_2\text{–Ti(III)–}X_2\text{–Ti(III)–}(C_5H_5)_2)$, where X = F, Cl, Br, and I have been investigated by Coutts *et al.* (*12*). The details of the crystal structure are only reported for X = Cl (*13*).

The geometry around each Ti^{3+} ion in $(Ti_2F_{10})^{4-}$ is highly distorted from octahedral, most notable is the considerable compression of the F9′–Ti–F9 angle (74.86°) and the corresponding opening of the Ti1–F9–Ti1 angle (105.14°). The interatomic distance between F9 and F9′ is 2.517 Å; the

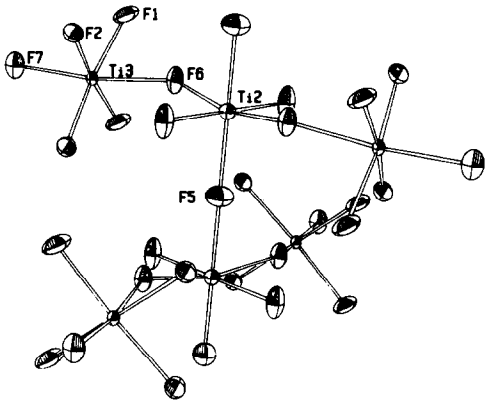

FIG. 2. Ti environment in the branched chains in $BaTiF_5$.

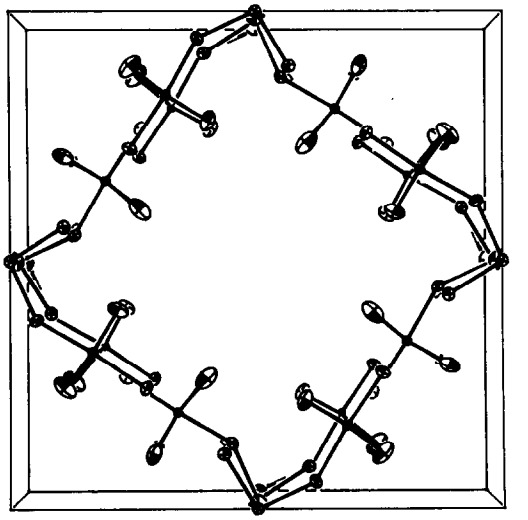

FIG. 3. Projection of chains onto (001) in $BaTiF_5$.

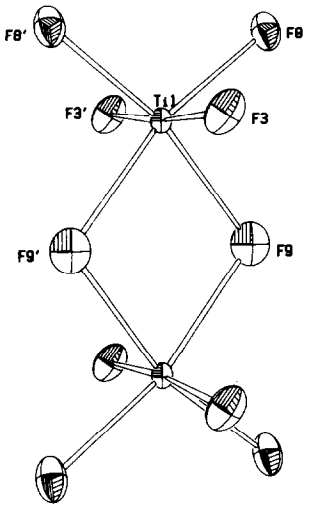

FIG. 4. Ti environment in the dimer in $BaTiF_5$.

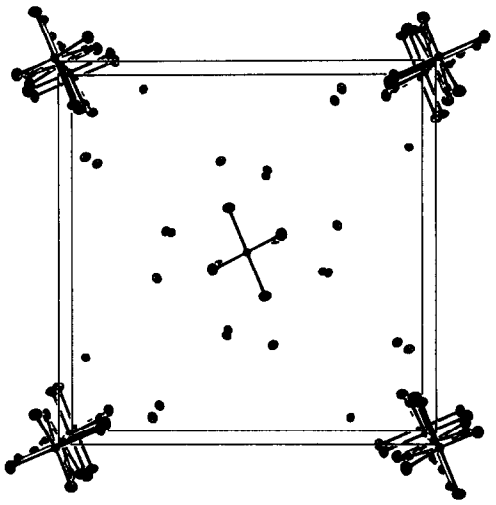

FIG. 5. Projection of dimers onto (001) in $BaTiF_5$.

separation of Ti^{3+} ions within a dimer is 3.288 Å, compared to a separation of 4.381 Å for Ti^{3+} ions belonging to different dimers. The Ti1–F9 bond distance is 2.070 Å. If the difference in the size of Cl^- (1.67 Å (*10*)) and F^- (1.145 Å (*10*)) is taken into account, these angles and distances compare well with those determined for the $(Ti_2Cl_2)^{4+}$ nucleus in $[(C_5H_5)_2TiCl]_2$ (*13*). For comparison these data are listed in Table VIII.

The dimers are stacked parallel to the *c*-axis at $0,0,z$ and $\frac{1}{2},\frac{1}{2},z$ to form a chain of dimers (Fig. 5). The Ti^{3+} ions occupy a site on the fourfold axis and the fluorines F3, F8, and F9 are disordered around this axis.

TABLE VIII

COMPARISON OF THE HALIDE-BRIDGES $(Ti_2X_2)^{4+}$ IN $BaTiF_5$ AND $[(C_5H_5)_2Ti\text{–}Cl]_2$ (*13*)

X	F	Cl
r_x (Å)	1.145	1.67
<*X*–Ti–*X* (°)	74.86(36)	77.11(5)
<Ti–*X*–Ti (°)	105.14(50)	102.89(5)
Ti–*X* (Å)	2.070(7)	2.540(2)
Ti–Ti (Å)	3.288(3)	3.968(2)

There are two possible orientations of the dimer, depending on whether the plane defined by F8, Ti1, and F9 is parallel to the *a* or *b* axis (Fig. 6). Within a chain of dimers the relative orientation of two neighboring $(Ti_2F_{10})^{4-}$ units with respect to each other is fixed, because of steric constraints. However, there is no communication between

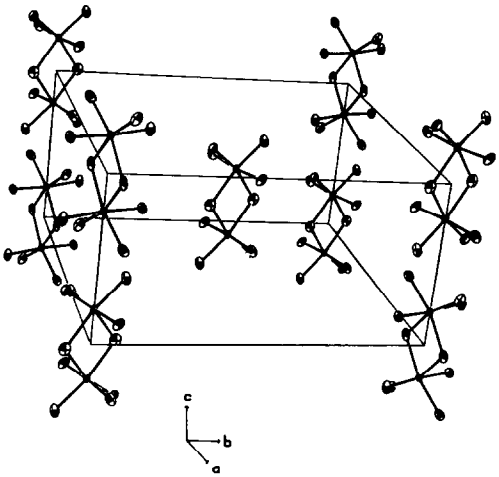

FIG. 6. Distribution of dimers in the unit cell of $BaTiF_5$, showing the two possible orientations of the dimers w.r.t the axes *a* and *b*.

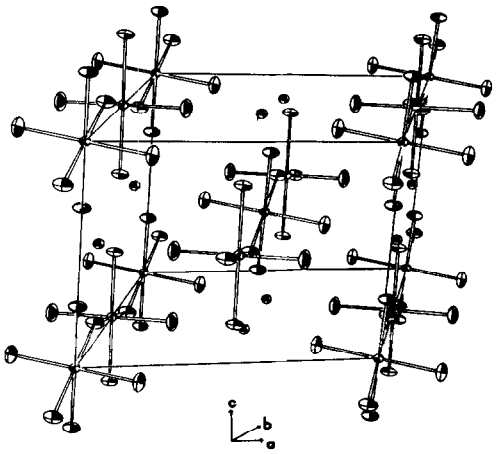

FIG. 7. Unit cell of $CaTiF_5$.

the chains and thus the orientation of two chains with respect to each other is random. This fact accounts for the observed rotational disorder of the fluorines F3, F8, and F9. In the $BaFeF_5$ structure, as reported, this chain of dimers is replaced by an infinite, linear chain of corner-sharing FeF_6 octahedra, i.e. $(FeF_5)_n^{2n-}$. It must be noted, however, that in $BaFeF_5$ (*3*) the Fe–Fe distances are also found to alternate between 3.48 and 4.13 Å. In addition, the bridging fluorines (F(2) and F(3), Ref. (*3*)), located between two Fe^{3+} ions, have temperature factors which are considerably larger than those of the other fluoride ions (with the exception of F(5)) in the structure. The results obtained for $BaTiF_5$ and the fact that the structure of $BaFeF_5$ was solved using film techniques (R_{final} = 0.102 for 290 reflections (*3*)), cast doubt on the presence of linear chains of FeF_6-octahedra in Ba FeF_5. The structure of $BaFeF_5$ bears reinvestigation.

The possibility that the $(Ti_2F_{10})^{4-}$ dimers would break up and form chains on raising the temperature was investigated by differential scanning calorimetry (DSC). No thermal effects were observed up to the melting point at 890 ± 20°C, indicating that the dimers stay intact.

(*ii*) *$CaTiF_5$*. This compound is isostructural with $CaCrF_5$ (*5, 6*) and $MnCrF_5$ (*9*); a diagram of the unit cell is shown in Fig. 7. The structure is characterized by linear chains of TiF_6-octohedra, $(TiF_5)_n^{2n-}$, propagating parallel to the *c*-axis. Each TiF_6 octahedron is tilted w.r.t. its neighbor, the Ti–F–Ti angle is 145.48(8)°. The arrangement around the Ti^{3+} ion is again distorted from a regular octahedron (Fig. 8, Table V). The Ti–F bond lengths (*l*) are in the range 1.886 $\leq l \leq$ 2.015 Å and compare well with the sum of the ionic radii (2.010 Å (*10*)). The Ca^{2+} ion is surrounded by seven fluorine atoms at the vertices of a pentagonal bipyramid (Fig. 9, Table V).

Magnetic Study

The magnetic data obtained for $CaTiF_5$ and $BaTiF_5$ (Fig. 1) show no evidence for either long- or short-range magnetic order. These results are in contrast to the observations made for the related compounds $CaMF_5$ (*M* = Cr,Fe)(2) which behave as 1-D antiferromagnets with exchange constants of −3.85 and −10.8 K, respectively. For $BaMF_5$ (*M* = V,Fe) 3-D antiferromagnetic order was found to set in at 20 and 35 K, respectively (11); a weak ferromagnetic component developed below T_N. In the Ti-compounds the superexchange interaction is apparently not strong enough to cause ordering of the Ti-moments at temperatures

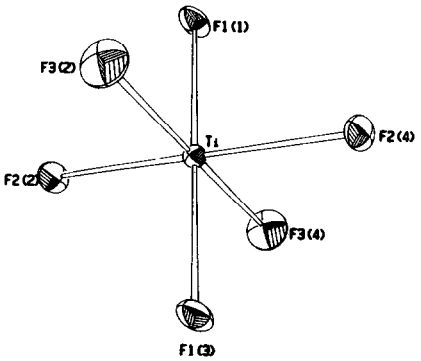

FIG. 8. Ti^{3+} environment in $CaTiF_5$.

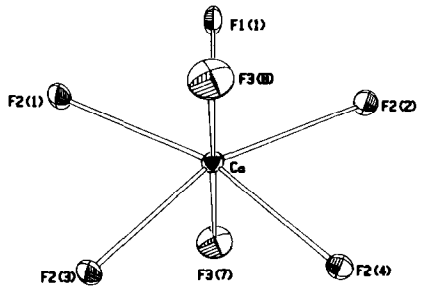

FIG. 9. Ca^{2+} environment in $CaTiF_5$.

above 4.2 K. Figure 1 shows the inverse susceptibility of $BaTiF_5$ and $CaTiF_5$ as a function of temperature. The remarkable feature of these graphs is their strong curvature at high T, which is thought to be the result of crystal field effects.

An attempt was made to understand the T-variation of the susceptibility in terms of a simplified model for the crystal field interaction and van Vleck's equation. The crystallographic site symmetry at Ti^{3+} in the compounds under investigation is quite low: $(\bar{1})$ for Ti in $CaTiF_5$, $(2/m)$ for Ti2 and (m) for Ti3 in $BaTiF_5$. The correct crystal field (CF) Hamiltonian for any of these cases would contain a large number of terms, making it difficult to treat the problem exactly. We then assumed the ion site to have predominantly cubic symmetry with components of lower symmetry. Thus, the total Hamiltonian was written:

$$H = H_{CF}^{Cubic} + H_{CF}^{Noncubic} + H_{SO} + H_{MAG}$$

and the spin-orbit coupling (H_{SO}) and noncubic CF part were treated as simultaneous perturbations, with the overall Hamiltonian being diagonalized in the basis of the cubic crystal field states. $H_{CF}^{Noncubic}$ was restricted to $B_2^0O_2^0 + B_2^2O_2^2$ using the formalism of Stevens (*14*). Initial values of B_2^0 and B_2^2 were obtained from lattice-sum, point-charge calculations, and the actual values tried varied over a wide range. Unfortunately, no choice of parameters resulted in satisfactory agreement between calculated and experimental susceptibilities. This lack of agreement reflects, presumably, the inadequacy of our model for the crystal field.

In place of the more detailed analysis, the χ^{-1} vs T curves were analyzed in terms of the Curie–Weiss law plus a temperature-independent term (χ_{TIP}):

$$\chi = \frac{C}{T - \theta} + \chi_{TIP}$$

This approach is consistent with the overall shape of the χ^{-1} vs T curves for both materials which suggest a magnetic ground doublet for Ti^{3+} separated by only a few tens of a Kelvin from a low-lying excited doublet or doublets which contribute a van Vleck susceptibility. The parameters obtained from a nonlinear least squares fit to this function are listed in Table VI. In this simple approach the molar Curie constant can be related to the number of paramagnetic spins in the sample. In $BaTiF_5$ one-quarter of the Ti^{3+} ions are coupled into dimers and assuming a singlet ground state for the dimer these Ti^{3+} ions will not contribute to the magnetic susceptibility of the material to first order. The Curie constant of $BaTiF_5$ is expected to be 0.75 $C_{FREE\ ION}$ (Ti^{3+})/F.U. (0.280). The observed value of 0.200(13) is even smaller than this estimate. Apart from lowering the Curie constant, the presence of the Ti^{3+} dimers should make a significant contribution to the temperature-independent paramagnetism, χ_{TIP}. Comparison of χ_{TIP} obtained for $CaTiF_5$ and $BaTiF_5$ reveals that indeed χ_{TIP} ($BaTiF_5$) is considerably larger than χ_{TIP} ($CaTiF_5$). The paramagnetic Curie temperatures (θ) for both compounds were found to be rather small.

In summary, the magnetic behavior of $CaTiF_5$ and $BaTiF_5$ is characterized by the absence of magnetic interactions. Both materials have substantial temperature-independent contributions to the magnetic sus-

ceptibility which are thought to arise as a consequence of crystal field effects alone as for $CaTiF_5$ or augmented by a component from Ti^{3+} dimers in the case of $BaTiF_5$.

Acknowledgments

We thank Professor W. Boo for performing the magnetic susceptibility measurements. Furthermore, we thank Mr. R. Faggiani for collecting the X-ray diffraction data and his advice in the course of structure determination; Professor C. J. L. Lock and Mr. J. Britten for many helpful discussions. The technical assistance of Mr. J. D. Garrett and Mr. F. Gibbs are gratefully acknowledged. This work received financial support from the National Science and Engineering Council of Canada and McMaster University (S.E.).

References

1. A. Tressaud and J. M. Dance, *Advan. Inorg. Radiochem.* **20,** 133 (1977).
2. J. M. Dance, J. L. Soubeyroux, L. Fournes, and A. Tressaud, *C. R. Acad. Sci. Paris C* **288,** 37 (1979).
3. R. Von der Mühll, S. Anderson, and J. Galy, *Acta Crystallogr. B* **27,** 2345 (1971).
4. R. Von der Mühll and J. Ravez, *Rev. Chim. Miner.* **11,** 652 (1974).
5. D. Dumora, R. Von der Mühll, and J. Ravez, *Mater. Res. Bull.* **6,** 561 (1971).
6. Kang Ku Wu and I. D. Brown, *Mater. Res. Bull.* **8,** 593 (1973).
7. A. C. Larson, *Acta Crystallogr.* **23,** 664 (1967).
8. (a) D. T. Cromer and J. T. Waber, "International Tables for X-Ray Crystallography," Vol. IV, Table 2.2A, p. 72 ff.; (b) D. T. Cromer, Table 2.3.1, pp. 149–150, Kynoch Press, Birmingham, England (1974).
9. G. Ferey, R. de Pape, M. Poulain, D. Grandjean, and A. Hardy, *Acta Crystallogr. B* **33,** 1409 (1977).
10. R. D. Shannon, *Acta Crystallogr. A* **32,** 751 (1976).
11. R. Georges, J. Ravez, R. Olazcuaga, and P. Hagenmuller, *J. Solid State Chem.* **9,** 1 (1974).
12. R. S. P. Coutts, R. L. Martin, and P. C. Wailes, *Aust. J. Chem.* **26,** 2101 (1973).
13. R. Jungst, D. Sekutowski, J. Davis, M. Luly, and G. Stucky, *Inorg. Chem.* **16,** 1645 (1977).
14. K. W. H. Stevens, *Proc. Phys. Soc. (London) A* **65,** 542 (1952).